Cell Metabolism
Article

Endoplasmic Reticulum Stress Plays a Central Role in Development of Leptin Resistance

Lale Ozcan,[1,4] Ayse Seda Ergin,[1,4] Allen Lu,[1] Jason Chung,[1] Sumit Sarkar,[1] Duyu Nie,[2] Martin G. Myers, Jr.,[3] and Umut Ozcan[1,*]
[1]Division of Endocrinology
[2]Division of Neurology
Children's Hospital Boston, Harvard Medical School, Boston, MA, 02115, USA
[3]Division of Metabolism, Endocrinology, and Diabetes, Department of Medicine, University of Michigan Medical School, Ann Arbor, MI, 48109, USA
[4]These authors contributed equally to this work
*Correspondence: umut.ozcan@childrens.harvard.edu
DOI 10.1016/j.cmet.2008.12.004

SUMMARY

Leptin has not evolved as a therapeutic modality for the treatment of obesity due to the prevalence of leptin resistance in a majority of the obese population. Nevertheless, the molecular mechanisms of leptin resistance remain poorly understood. Here, we show that increased endoplasmic reticulum (ER) stress and activation of the unfolded protein response (UPR) in the hypothalamus of obese mice inhibits leptin receptor signaling. The genetic imposition of reduced ER capacity in mice results in severe leptin resistance and leads to a significant augmentation of obesity on a high-fat diet. Moreover, we show that chemical chaperones, 4-phenyl butyric acid (PBA), and tauroursodeoxycholic acid (TUDCA), which have the ability to decrease ER stress, act as leptin-sensitizing agents. Taken together, our results may provide the basis for a novel treatment of obesity.

INTRODUCTION

The epidemic surge in the prevalence of obesity is one of the most serious public health problems confronting the western societies. Among the adult population in the United States, 65% is overweight and more than 30% is obese (Stein and Colditz, 2004). There has also been an increase in the obese pediatric population, with one out of three Americans born in the year 2000 expected to suffer from the complications of obesity in their later lifetime (Narayan et al., 2003; Rocchini, 2002). Although causally linked to debilitating conditions such as insulin resistance, type 2 diabetes, atherosclerosis, and cardiovascular disease, there remains limited effective therapeutic treatment for obesity (Muoio and Newgard, 2006).

Leptin is an adipocyte-derived hormone that suppresses appetite mainly through its action on a subset of hypothalamic neurons (Halaas et al., 1995; Leibel et al., 1997). It also allows the body to expend energy necessary for growth, reproduction, and immunity (Ahima et al., 1996; Friedman and Halaas, 1998). Genetic leptin deficiency in mice and humans leads to a severe form of monogenic obesity due to unregulated appetite and reduced energy expenditure (Farooqi and O'Rahilly, 2005; Gao and Horvath, 2007; Proulx and Seeley, 2005). The discovery of leptin more than a decade ago created hope that it might be used therapeutically in the treatment of obesity; however, except for rare leptin-deficient individuals, both diet-induced rodent models of obesity and obese humans are minimally responsive to leptin due to the development of leptin resistance in the brain and defects in transportation of leptin across the blood brain barrier (Banks, 2004; Elmquist et al., 1999; Flier, 2004; Schwartz and Morton, 2002; Schwartz et al., 2000). The molecular mechanisms of leptin resistance are poorly understood. Suppressor of cytokine signaling 3 (SOCS3) (Bjorbak et al., 2000; Flier, 2004; Myers, 2004) and tyrosine phosphatase 1 B (PTB1B) have been shown to play important roles in the blockade of leptin signaling (Bence et al., 2006). In addition, recent evidence has demonstrated that increased serine phosphorylation of Janus kinase 2 (Jak2) contributes to the blockade of leptin action (Ishida-Takahashi et al., 2006).

The endoplasmic reticulum (ER) is a sophisticated luminal network in which protein synthesis, maturation, folding, and transport take place (Marciniak and Ron, 2006; Schroder and Kaufman, 2005). Perturbation of these processes in several different pathological states creates a condition defined as ER stress and leads to activation of a complex signaling network termed the unfolded protein response (UPR) (Ron and Walter, 2007). Previous studies have demonstrated that ER stress and activation of UPR signaling pathways play a dominant role in the development of obesity-induced insulin resistance and type 2 diabetes (Ozcan et al., 2004). Furthermore, reversal of ER stress with chemical chaperones—agents that have the ability to increase ER folding machinery—increases insulin sensitivity and reverses type 2 diabetes in obese mice (Ozcan et al., 2006). The mechanisms underlying ER stress and activation of UPR signaling in obesity are not completely understood. Current evidence suggests that increased levels of circulating cytokines, free fatty acids (FFA), exposure to excess nutrition, and subsequent activation of the mammalian target of rapamycin (mTOR) pathway (Ozcan et al., 2006, 2008; Ron and Walter, 2007) contribute to the development of ER stress and activation of UPR signaling pathways.

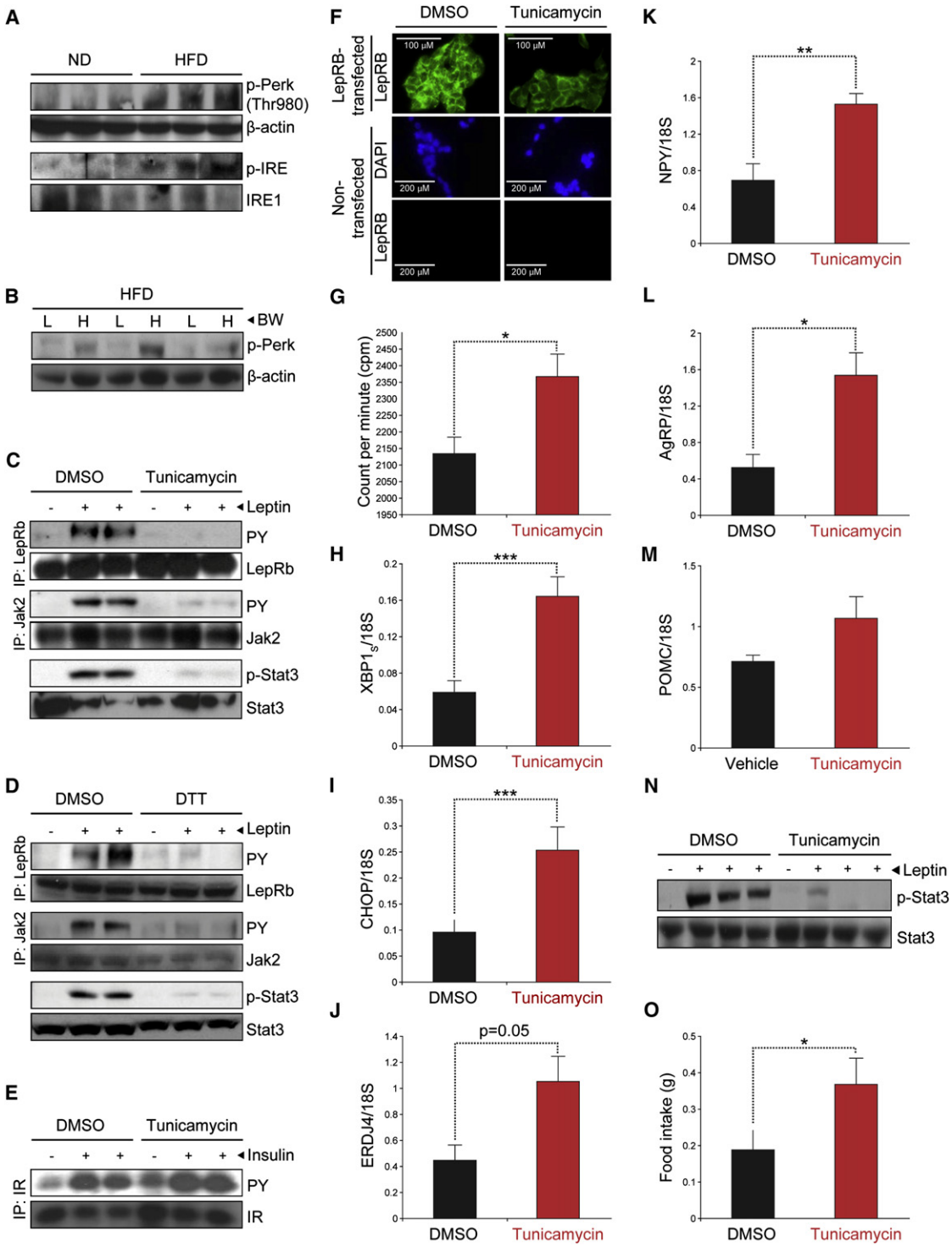

Figure 1. UPR Parameters in Hypothalamus of HFD-Fed Obese Mice

(A) UPR signaling elements phospho-PERK (Thr980) and phospho-IRE1α (Ser724) were analyzed in the hypothalamus of the male C57BL/6 WT mice fed a normal or high-fat diet for a period of 25 weeks. (Blots are representative of three independent experiments.)

(B) PERK phosphorylation (Thr980) in the hypothalamus of the obese and nonobese HFD-fed C57BL/6 WT mice. (Blots are representative of one experiment with three different individual mice in each group.)

(C) LepRB-expressing 293 cells were either incubated with vehicle or tunicamycin (3 μg/ml) for 4 hr and subsequently taken to leptin (100 ng/ml) stimulation for 45 min. Leptin-stimulated tyrosine phosphorylation of long-form of leptin receptor (LepRB), Janus Kinase 2 (Jak2), and signal transducers and activators of transcription 3 (Stat3) (Tyr705) has been examined. (Blots are representative of more than three independent experiments.)

Mice engineered to have reduced ER capacity (Ozcan et al., 2004) or increased levels of ER stress (Scheuner et al., 2005) develop a higher degree of obesity when challenged with a high-fat diet. Because leptin-receptor-expressing neurons of the hypothalamus are exposed to ER-stress-associated factors such as increased FFAs and other nutrients (Myers, 2008), we have sought to determine whether ER system is perturbed within the hypothalamus and may contribute to the phenomenon of leptin resistance and, in turn, to obesity itself.

RESULTS

Increased ER Stress in Hypothalamus of Obese Mice

To examine whether obesity creates ER stress in the hypothalamus, we analyzed PERK phosphorylation in hypothalamus extracts of mice fed a normal diet (ND) or high-fat diet (HFD) for a period of 20 weeks. PERK phosphorylation (Thr 980) was significantly increased in hypothalami of the HFD-fed mice when compared with ND-fed mice (Figure 1A), indicating to a state of activated UPR. β-actin immunoblotting was performed in the same hypothalamic extracts to confirm that protein concentration is equal between the hypothalamic protein samples. To demonstrate that antiserum that we used to analyze PERK phosphorylation is specific, we treated the WT and *PERK*$^{-/-}$ mouse embryo fibroblasts with tunicamycin and analyzed PERK^{Thr980} phosphorylation. As shown in Figure S1 available online, the antibody specifically recognizes the phosphorylated PERK at Thr980 residue. To investigate whether IRE1 was also activated in the hypothalami of the HFD group, we analyzed IRE1 phosphorylation levels at Ser723, a phosphorylation site previously shown to correlate with increased IRE1 activity. There was a significant increase in IRE1 phosphorylation in the hypothalami of HFD-fed group when compared with the ND-fed lean group (Figure 1A). Taken together, the data presented above indicate that obesity creates ER stress in the hypothalamus. Indeed, a recent publication has also demonstrated that PERK phosphorylation is increased in the hypothalamus of the obese mice (Zhang et al., 2008).

To examine whether ER stress generally occurs in the hypothalamus of the HFD-fed mice regardless of obesity or mainly develops in the mice, which develops obesity, we placed a cohort of C57BL/6 male mice on HFD at the age of 3 weeks. Following 8 weeks of HFD feeding, we chose the mice with high and low body weights and analyzed the PERK phosphorylation in hypothalamus extracts of these mice. PERK phosphorylation is markedly upregulated in the hypothalami of the mice that have developed obesity, but not in the group that has not developed obesity (Figure 1B). These results indicate that development of obesity correlates with the development of ER stress in the hypothalamus.

ER Stress Inhibits Leptin Receptor Signaling

The long form of leptin receptor (LepRB) has been shown to mediate the anorexigenic effect of leptin in the central nervous system. To examine whether UPR might alter the leptin signaling, LepRB-expressing 293 cells were first exposed to tunicamycin (3 μg/ml) to activate ER stress for a period of 4 hr and then treated with leptin (100 ng/ml) for 45 min. Stimulation of DMSO-treated 293 cells with leptin led to a marked increase in LepRB tyrosine phosphorylation (Figure 1C). However, pretreatment of the cells with tunicamycin completely inhibited leptin-stimulated tyrosine phosphorylation of LepRB without altering the total protein levels (Figure 1C). Next, we analyzed Jak2 tyrosine phosphorylation; as with LepRB, the leptin-stimulated Jak2 tyrosine phosphorylation was reduced to an undetectable level when the cells were subjected to ER stress (Figure 1C). Finally, as a downstream element, leptin-stimulated Stat3 activation was analyzed. As previously reported (Kloek et al., 2002), stimulation of 293 cells with leptin led to a significant increase in Stat3 phosphorylation at tyrosine 705 (Figure 1C). In contrast, when challenged with tunicamycin, the leptin-induced Stat3 phosphorylation (Tyr705) was totally abolished (Figure 1C), indicating that UPR signaling inhibits LepRB signaling at all steps. The same experiments were repeated with dithiothreitol (DTT), another commonly used ER stress-inducing agent, to prove that tunicamycin-mediated blockade was not due to nonspecific effects created by this agent (Figure 1D). Taken together, these results suggest that activation of UPR signaling pathways blocks leptin receptor signaling.

To exclude the possibility that LepRB-expressing 293 cells become dysfunctional due to a possible toxicity generated by tunicamycin, we investigated the insulin receptor (IR) activation by stimulating the cells with insulin (100 nM) for 5 min after 5 hr tunicamycin (3 μg/ml) treatment. During the 5 hr stimulation

(D) Analysis of LepRB signaling at the presence or absence of dithiothreitol (DTT) (1 mM). (Blots are representative of three independent experiments.)
(E) Insulin-stimulated insulin receptor (IR) activation in LepRB-expressing 293 cells after 5 hr DMSO or tunicamycin (3 μg/ml) stimulation. (Blots are representative of two independent experiments.)
(F) LepRB staining in 5 hr DMSO or tunicamycin-treated LepRB-expressing 293 cells or in the nontransfected 293 cells. (Pictures are representative of three independent experiments.)
(G) Binding of iodinated-leptin to LepRB after 5 hr of DMSO or tunicamycin stimulation. (Graph is representative of two independent experiments, and, in each of the experiments, n = 3 for the given conditions.)
(H) A 26 gauge guide cannula was implanted into the third ventricle of the lean, 8-week-old C57BL/6 mice. Following a 7 day healing period, either vehicle or tunicamycin (40 mg/ml, 2 μl) was infused to the third ventricle. At 12 hr following the infusion, hypothalamus was dissected. mRNA levels of spliced X box binding protein 1 (XBP1s), (I) CCAAT/enhancer-binding protein-homologous protein (CHOP), and (J) endoplasmic reticulum-resident DNAJ 4 (ERDJ4) in the hypothalamus of vehicle- or tunicamycin-infused mice.
(K) Neuropeptide Y (NPY), (L) agouti-related peptide (AgRP), and (M) pro-opiomelanocortin (POMC) mRNA levels in the hypothalamus of the control and tunicamycin-infused mice.
(N) Third ventricles of the 8-week-old C57BL/6 mice were infused with vehicle or tunicamycin. Leptin (1 mg/kg) was administered intraperitoneally 5.5 hr after the infusions, and phospho-Stat3 (Tyr705) and total Stat3 levels were determined within the hypothalamic protein samples.
(O) Food intake between 4 and 6 hr after tunicamycin infusion to the third ventricle. Graphs are representative of three independent experiments (n = 3 in each experiment).
Error bars, ± SEM. p values are determined by Student's t test. *$p < 0.05$; **$p < 0.01$; ***$p < 0.001$.

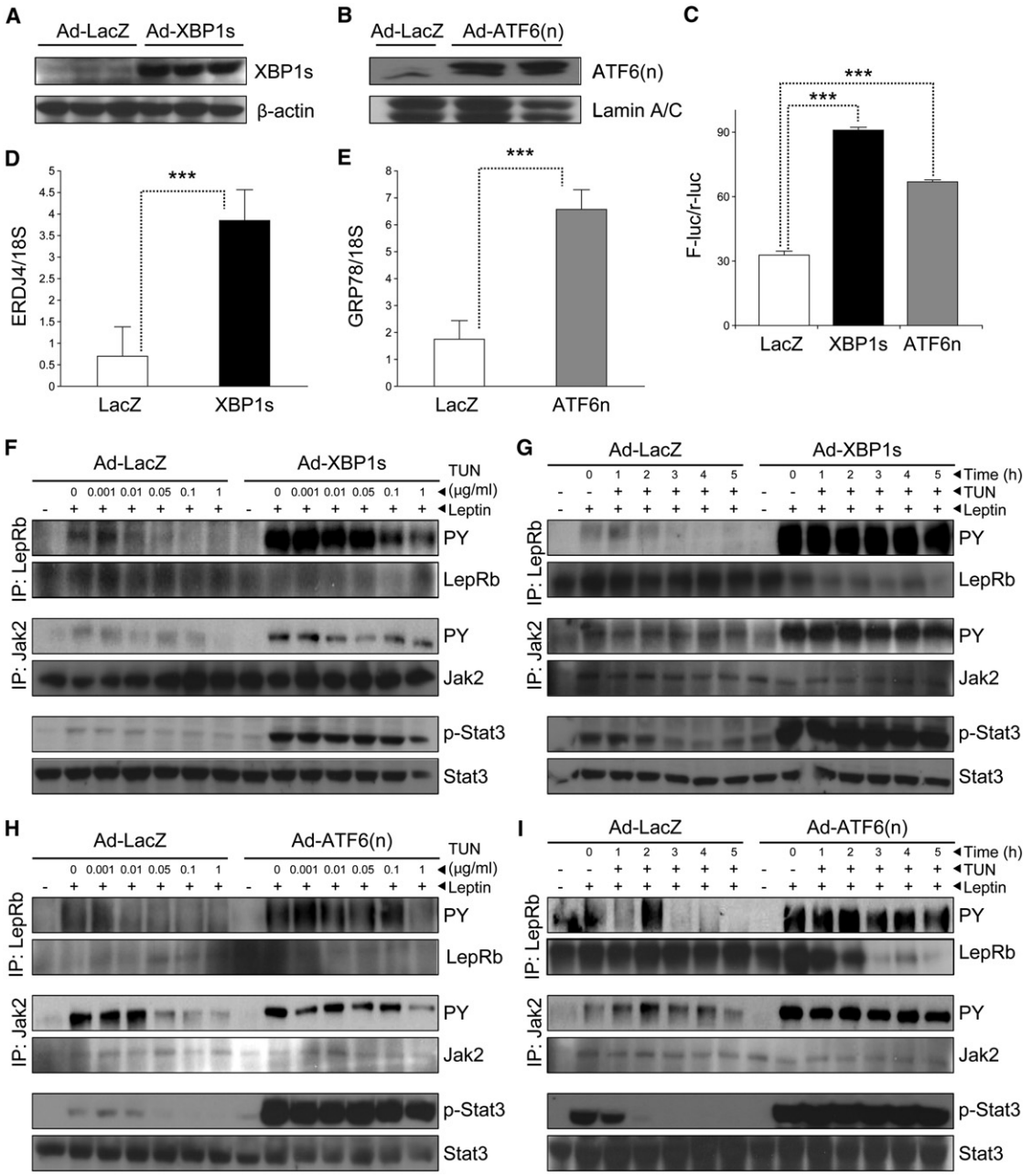

Figure 2. Improved ER Capacity Enhances Leptin Sensitivity

(A and B) Immunoblots of (A) XBP1s in the total cell lysates and (B) NH_2 terminal of ATF6 (ATF6n) in nuclear extracts of the mouse embryonic fibroblasts (MEFs) infected with adenovirus encoding either XBP1s (Ad-XBP1s) or ATF6n (Ad-ATF6n), respectively. (Both of the experiments in [A] and [B] were repeated independently three times.)

(C) Relative activity of the endoplasmic reticulum stress element (ERSE)-driven luciferase reporter after LacZ, XBP1s, and ATF6n expression. (Graph is representative of three independent experiments.)

(D and E) Relative expression levels of (D) ERDJ4 and (E) GRP78 after LacZ and XBP1s adenovirus infection. (Graph is representative of three to five independent experiments in different cellular systems.)

(F) LepRB-expressing 293 cells were infected with the Ad-LacZ and Ad-XBP1s, and following overnight starvation, cells were stimulated with increasing doses of tunicamycin (0.001, 0.01, 0.05, 0.1, 1 μg/ml) for 5 hr. Leptin was added to the medium at the last 45 min of the tunicamycin stimulation. Tyrosine phosphorylations of LepRB, Jak2 and Stat3 (Tyr705) and their total protein levels were analyzed.

(G) The 293 cells expressing either LacZ or XBP1s were incubated with tunicamycin (0.05 μg/ml) in a time course manner up to 5 hr after an overnight starvation and exposed to leptin (100 ng/ml) for additional 45 min. LepRB and Jak2 tyrosine phosphorylations were investigated after immunoprecipitation, and Stat3 (Tyr705) phosphorylation has been examined with direct immunoblotting in whole-cell lysates.

(H) Following infection with Ad-ATF6n, 293 cells were incubated in 1% FBS containing medium for 14 hr and then stimulated with increasing doses of tunicamycin (0.001, 0.01, 0.05, 0.1, and 1 μg/ml) for 5 hr. Cells were given leptin (100 ng/ml) stimulation at the last 45 min of the tunicamycin incubation. LepRB and Jak2

period, insulin-stimulated IR tyrosine phosphorylation did not change, which supports the observation that LepRB-expressing 293 cells are functional during the experimental time frame that we used (Figure 1E).

Considering the fact that LepRB is folded in the ER, we investigated whether ER stress blocks leptin receptor translocation to the membrane from the ER and whether this could be a reason for the blockade of leptin signaling. We stimulated the 293 cells with tunicamycin for 5 hr (3 μg/ml) and analyzed leptin receptor levels in the plasma membrane by immunofluorescence staining. As shown in Figure 1F, LepRB folding is still preserved, and its translocation to the membrane is not decreased in ER stress conditions. Next, we performed leptin-binding assays in DMSO and tunicamycin-treated cells to exclude the possibility of a defect in binding of leptin to LepRB. Surprisingly, leptin binding to LepRB significantly increased in ER stress conditions (Figure 1G).

ER Stress Creates Leptin Resistance in the Brain of Lean Mice

To investigate whether leptin action could also be blocked by directly inducing ER stress in brains of lean mice, we inserted a guide cannula to the third ventricle and infused tunicamycin and vehicle as control. mRNA levels of ER-stress-responsive genes such as the spliced form of X box binding protein 1 (XBP1s), CCAAT/enhancer-binding protein-homologous protein (CHOP), and endoplasmic reticulum resident DNAJ 4 (ERDJ4) were significantly upregulated in hypothalami of tunicamycin-infused mice (Figures 1H, 1I, and 1J), indicating that ER stress can be induced in the hypothalamus of lean mice by tunicamycin infusion.

Next, we investigated the expression patterns of leptin resistance markers such as neuropeptide Y (NPY) and agouti-related peptide (AgRP) in the vehicle- and tunicamycin-infused mice. Induction of ER stress in the brain of the lean mice led to a significant increase in the mRNA levels of NPY and AgRP, indicating a leptin-resistant state (Figures 1K and 1L). The POMC mRNA levels did not show any significant difference in the tunicamycin-infused hypothalami (Figure 1M). In addition, to exclude the possibility that tunicamycin infusion leads to a decay in mRNA degradation of NPY and AgRP due to a possible toxic effect, we analyzed mRNA levels of IR and insulin receptor substrate 1 (IRS1) (Figures S1A and S1B).

To assess whether activation of UPR signaling would create leptin resistance and block the leptin-stimulated Stat3 activation in the hypothalamus, leptin (1 mg/kg/day) was intraperitoneally administered 5.5 hr after tunicamycin infusion. IP administration of leptin led to a marked increase in Stat3 phosphorylation in the hypothalamus (Figure 1N). In contrast, administration of tunicamycin to the third ventricle and creation of ER stress, in complete accordance with our data obtained from 293 cells, blocked activation of Stat3 in the hypothalamus (Figure 1N). Furthermore, infusion of tunicamycin to the third ventricle significantly increased acute food intake (Figure 1O).

Improvement of ER Function Enhances Leptin Signaling

XBP1s is one of the master regulators of ER folding capacity (Ron and Walter, 2007; Schroder and Kaufman, 2005). To determine whether exogenous expression of XBP1s and a consequent increase in ER function would enhance leptin receptor signaling, we generated an XBP1s-encoding adenovirus (Ad-XBP1s) and also a LacZ-expressing adenovirus (Ad-LacZ) as a control. Infection of mouse embryonic fibroblasts (MEFs) with Ad-XBP1s increased the protein level of XBP1s (Figure 2A), upregulated ERSE promoter activity (Figure 2C), and increased the ERDJ4 mRNA levels (Figure 2D). After showing that newly generated Ad-XBP1s is functional, we subsequently overexpressed the XBP1s in the LepRB-expressing 293 cells and performed two sets of experiments. First, we stimulated the 293 cells with increasing doses of tunicamycin (0.001, 0.01, 0.05, 0.1, and 1 μg/ml) for 5 hr and analyzed leptin-stimulated LepRB activation. In Ad-LacZ infected cells, LepRB activation was blocked at tunicamycin doses of 0.01 μg/ml and higher (Figure 2F). In contrast, infection with Ad-XBP1s led to a marked increase in leptin-stimulated LepRB tyrosine phosphorylation even at the basal state, without altering the LepRB activation at the absence of leptin. XBP1s overexpression increased the resistance of cells to the inhibitory effect of tunicamycin of up to 0.05 μg/ml. Even at the doses of 0.1 and 1 μg/ml of tunicamycin, leptin-stimulated activation of LepRB in XBP1s overexpressing cells was higher than the LacZ-expressing cells in the absence of tunicamycin (Figure 2F). Both 0.01 and 0.05 μg/ml of tunicamycin concentration significantly induces ER stress and upregulates CHOP expression in the 293 cells (Figure S1C).

In the second set of experiments, we performed time course tunicamycin stimulation to determine at which time points the leptin receptor activity begins to decay. When Ad-LacZ infected 293 cells were treated with 0.05 μg/ml dose of tunicamycin, leptin-stimulated LepRB and Jak2 activation, as well as Stat3 tyrosine phosphorylation, were blocked within 2 hr. In contrast, overexpression of XBP1s prevented the ER stress-mediated blockade of LepRB, Jak2, and Stat3 tyrosine phosphorylations throughout the experimental period (Figure 2G).

If the increased leptin sensitivity after XBP1s expression was due to enhanced ER capacity, then another means of upregulating ER capacity should similarly enhance LepRB activation. Activating transcription factor 6α (ATF6) belongs to the bZIP transcription factor family and is also a fundamental regulator of ER adaptive capacity (Ron and Walter, 2007). Accordingly, we constructed adenovirus expressing the NH_2-terminal (1–373 aa) of ATF6α (Ad-ATF6n). Following the characterization of the adenovirus (Figures 2C and 2E), we infected the LepRB-expressing 293 cells with Ad-ATF6n and performed dose curve

immunoprecipitates were immunoblotted with a phosphotyrosine antibody, and Stat3 tyrosine phosphorylation was analyzed with a phosphospecific antibody raised against tyrosine 705.

(I) LacZ and ATF6n-infected 293 cells were taken to time course (1, 2, 3, 4, and 5 hr) tunicamycin (0.05 μg/ml) stimulation and stimulated with leptin (100 ng/ml) for 45 min. Subsequently, LepRB signaling parameters were analyzed.

Error bars, ± SEM. p values are determined by Student's t test. *$p < 0.05$, **$p < 0.01$, ***$p < 0.001$. Each experiment in (F–I) was repeated three times.

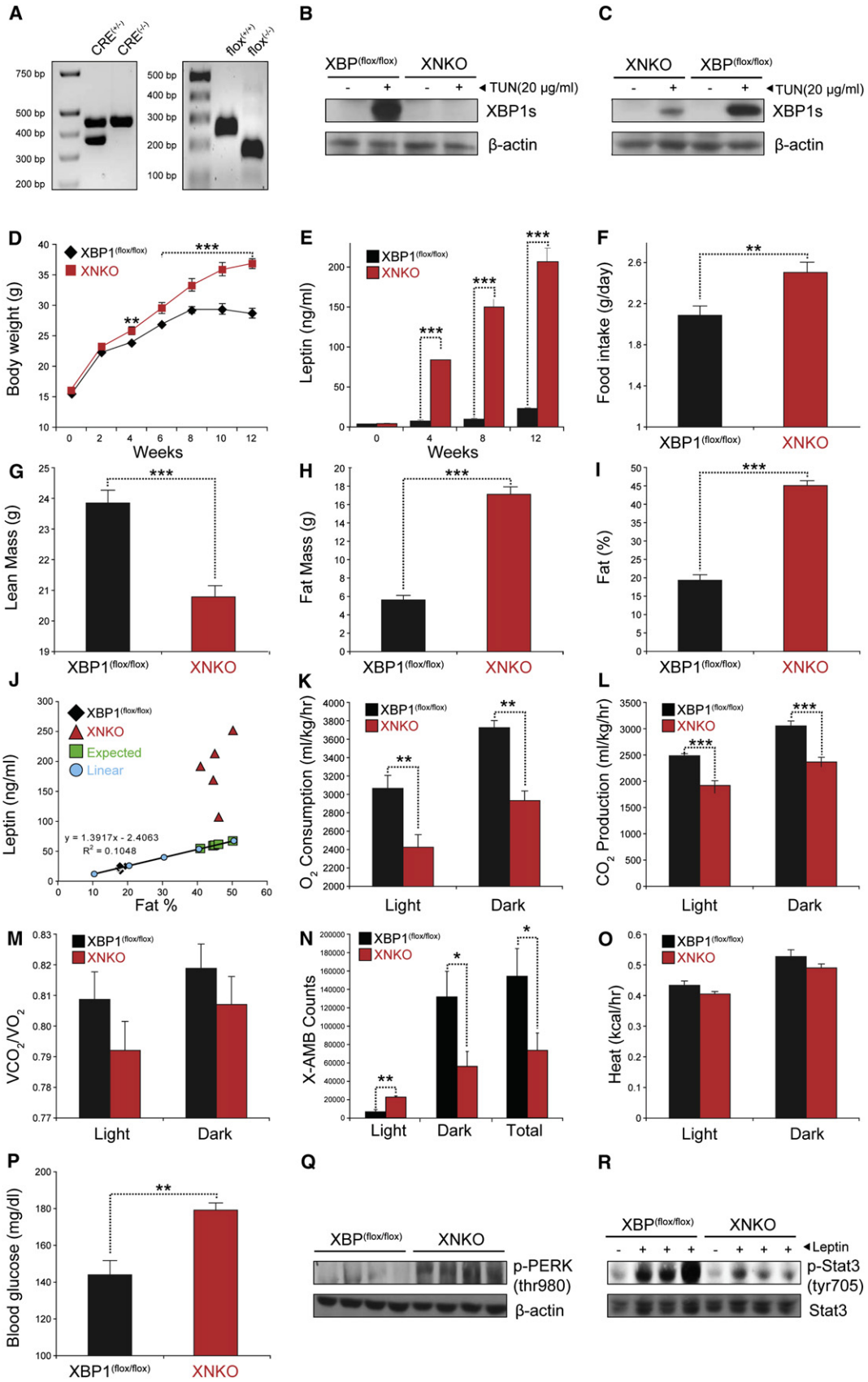
A
CRE(+/+)
CRE(-/-)
flox(+/+)
flox(-/-)
750 bp
500 bp
400 bp
300 bp
200 bp
500 bp
400 bp
300 bp
200 bp
100 bp
B
XBP(flox/flox)
XNKO
- + - + ◂TUN(20 μg/ml)
XBP1s
β-actin
C
XNKO
XBP(flox/flox)
- + - + ◂TUN(20 μg/ml)
XBP1s
β-actin
D
XBP1(flox/flox)
XNKO
Body weight (g)
Weeks
E
XBP1(flox/flox)
XNKO
Leptin (ng/ml)
Weeks
F
Food intake (g/day)
XBP1(flox/flox)
XNKO
G
Lean Mass (g)
XBP1(flox/flox)
XNKO
H
Fat Mass (g)
XBP1(flox/flox)
XNKO
I
Fat (%)
XBP1(flox/flox)
XNKO
J
XBP1(flox/flox)
XNKO
Expected
Linear
y = 1.3917x - 2.4063
R2 = 0.1048
Leptin (ng/ml)
Fat %
K
XBP1(flox/flox)
XNKO
O2 Consumption (ml/kg/hr)
Light
Dark
L
XBP1(flox/flox)
XNKO
CO2 Production (ml/kg/hr)
Light
Dark
M
XBP1(flox/flox)
XNKO
VCO2/VO2
Light
Dark
N
XBP1(flox/flox)
XNKO
X-AMB Counts
Light
Dark
Total
O
XBP1(flox/flox)
XNKO
Heat (kcal/hr)
Light
Dark
P
Blood glucose (mg/dl)
XBP1(flox/flox)
XNKO
Q
XBP(flox/flox)
XNKO
p-PERK
(thr980)
β-actin
R
XBP(flox/flox)
XNKO
- + + + - + + + ◂Leptin
p-Stat3
(tyr705)
Stat3

and time course tunicamycin treatment. Similar to the XBP1s, expression of ATF6n significantly upregulated the leptin-stimulated LepRB tyrosine phosphorylations at the basal conditions (Figure 2H). Similar to the results obtained from XBP1s gain-of-function experiments, ATF6n increased the resistance of 293 cells to tunicamycin and blocked the ER stress-mediated inhibition of LepRB signaling (Figures 2H and 2I).

ER Capacity of the Brain Links Obesity to Leptin Resistance

If the conditions that lead to development of obesity create perturbations in ER system and activate UPR signaling pathways, and if this signaling network plays a dominant role in the development of leptin resistance, it would be expected that a brain with a lower ER capacity, when exposed to the conditions that create obesity, will develop an earlier and higher degree of leptin resistance that will ultimately trigger the development of a more severe form of obesity. To test this hypothesis in vivo, we created neuron-specific XBP1 knockout mice (*XNKO*) by crossing the XBP1$^{flox/flox}$ mice with mice expressing Cre recombinase under the control of the nestin gene promoter. As previously reported (Hetz et al., 2008), *XNKO* mice are born in a Mendelian ratio and do not have any obvious phenotypic abnormality. Figure 3A shows the PCR analysis of floxed and Cre alleles of the *XNKO* and XBP1$^{flox/flox}$ mice. To demonstrate that XBP1 levels were reduced in the CNS and particularly in the hypothalamus of the *XNKO* mice, we have taken two different approaches. First, we exposed isolated embryonic cortical neurons to a high dose of tunicamycin (20 μg/ml) for a period of 6 hr. Exposure of XBP1$^{flox/flox}$ neurons to tunicamycin resulted in robust upregulation of the XBP1s protein levels (Figure 3B). However, this response is completely abolished in the neurons isolated from *XNKO* embryos, indicating that deletion of XBP1 is complete. Furthermore, we stimulated XBP1$^{flox/flox}$ and *XNKO* hypothalamic explants with tunicamycin (20 μg/ml) for 6 hr and demonstrated that there is a severe reduction in the protein levels of XBP1s in the *XNKO* hypothalamus (Figure 3C).

After showing that XBP1 can be significantly reduced in XBP1$^{flox/flox}$/*NesCre*$^{+/-}$ mice, we first analyzed the phenotype of the XBP1$^{flox/flox}$ and *XNKO* mice under normal diet feeding. The body weight of *XNKO* mice is slightly lower than the XBP1$^{flox/flox}$ mice under normal diet feeding conditions (Figure S2A). Blood glucose levels and leptin levels were similar during the experimental period for up to 12 weeks (Figures S2B and S2C). Performance of insulin (ITT) and glucose (GTT) tolerance tests showed that glucose homeostasis can be maintained under normal range in the *XNKO* mice under normal diet feeding (Figures S2D and S2E). Finally, we investigated the hypothalamic leptin receptor signaling by administering intraperitoneal leptin (1 mg/kg). Leptin-stimulated tyrosine phosphorylation of Stat3 does not show any difference between the *XNKO* and XBP1$^{flox/flox}$ control mice (Figure S2F), indicating that leptin action is preserved in the *XNKO* mice under normal diet feeding.

Next, we placed *XNKO* and XBP1$^{flox/flox}$ mice on high-fat diet at the age of 3.5 weeks, immediately after weaning. When challenged with HFD, *XNKO* mice gained more weight beginning at the second week and reached significantly higher levels of body weight by the fourth week (26.68 ± 0.64 g versus 23.53 ± 0.53, *XNKO* versus XBP1$^{flox/flox}$, $p = 0.002$). *XNKO* mice continued to gain weight at a more rapid rate than the control mice throughout the experimental period (Figure 3D).

Soon after initiation of HFD, leptin levels sharply increased in *XNKO* mice and reached 83.92 ± 8.2 ng/ml by the fourth week, corresponding to a 20-fold upregulation over the basal (pre-HFD) level (Figure 3E). The leptin levels continued to increase in *XNKO* mice during the course of the experiment and reached up to 50-fold higher levels (206.4 ± 17.56 ng/ml) by week 12 of HFD (Figure 3E). HFD feeding led to a much smaller increase in the leptin levels of the control XBP1$^{flox/flox}$ mice (Figure 3E). Additionally, measurement of 24 hr food intake at the twelfth week of HFD demonstrated that the *XNKO* group consumed more food than the XBP1$^{flox/flox}$ group (2.51 ± 0.09 g versus 2.08 ± 0.07 g, *XNKO* versus XBP1$^{flox/flox}$, $p < 0.01$) (Figure 3F). Performance of dual-energy X-ray absorptiometry (DEXA) scan has shown that the *XNKO* mice has significantly lower lean mass ($p < 0.001$) but a higher total fat amount when compared with the XBP1$^{flox/flox}$ mice ($p < 0.001$) (Figures 3G, 3H, and 3I). We performed a regression analysis to estimate the fat percentage-leptin level relationship in XBP1$^{flox/flox}$ mice, whose fat ranged between 15% and 20%. For *XNKO* mice, with fat percentage ranging between 45% and 50%, the regression would predict leptin levels around 60 ng/ml. Nonetheless, all five *XNKO* levels fell between 100 and 250 ng/ml, well above the prediction line (Figure 3J).

Figure 3. Deficiency of XBP1 in Neurons Increases Susceptibility to Develop Leptin Resistance

XBP1$^{flox/flox}$ mice on C57BL/6 background were intercrossed with the C57BL/6 mice that express the Cre recombinase under the nestin promoter.

(A) PCR analysis of the floxed and Cre alleles for genotyping.

(B) Cortical neurons were isolated from XBP1$^{flox/flox}$ and *XNKO* embryos at embryonic day ~15–~16. Following an overnight culture, neurons were stimulated with either DMSO or tunicamycin (20 μg/ml) for 6 hr, and XBP1s protein levels were analyzed with immunoblotting.

(C) Hypothalami were removed from the *XNKO* and XBP1$^{flox/flox}$ mice, dissected into small pieces, and incubated in basal neuron culture medium. Following 2 hr of incubation, tunicamycin (20 μg/ml) was added to the medium, and hypothalamic explants were treated with tunicamycin for 6 hr. XBP1s protein levels were analyzed with immunoblotting.

(D and E) (D) Body weight (g) and (E) plasma leptin (ng/ml) levels of XBP1$^{flox/flox}$ and *XNKO* mice during the course of high-fat diet feeding.

(F–J) (F) Regression analysis of leptin levels and fat percentage in the XBP1$^{flox/flox}$ and *XNKO* mice and (G) 24 hr food intake (g) at the twelfth week of HFD feeding. Dexa scan analysis of (H) lean mass (g), (I) total fat amount (g), and (J) fat percentage at the twelfth week of HFD feeding. Metabolic cage analysis was performed on XBP1$^{flox/flox}$ and *XNKO* mice at the eleventh week of HFD feeding.

(K–P) (K) O_2 consumption (ml/kg/hr), (L) CO_2 production (ml/kg/hr), (M) respiratory exchange ratio (VCO_2/VO_2), (N) x axis ambulatory activity, (O) heat generation (kcal/hr), and (P) blood glucose levels (mg/dl) at the twelfth week of HFD.

(Q) Hypothalamic PERK phosphorylation (Thr 980) in the XBP1$^{flox/flox}$ and *XNKO* mice at the thirteenth week of HFD.

(R) Leptin (IP, 1 mg/kg)-stimulated phosphorylation of Stat3 (Tyr705) in the XBP1$^{flox/flox}$ and *XNKO* mice at the thirteenth week of HFD.

n = 6 for *XNKO* group, and n = 11 for XBP1$^{flox/flox}$ group. The phenotype that has been observed in *XNKO* mice has been reproduced in two additional independent cohorts. Error bars, ± SEM. p values are determined by Student's t test. *$p < 0.05$, **$p < 0.01$, ***$p < 0.001$.

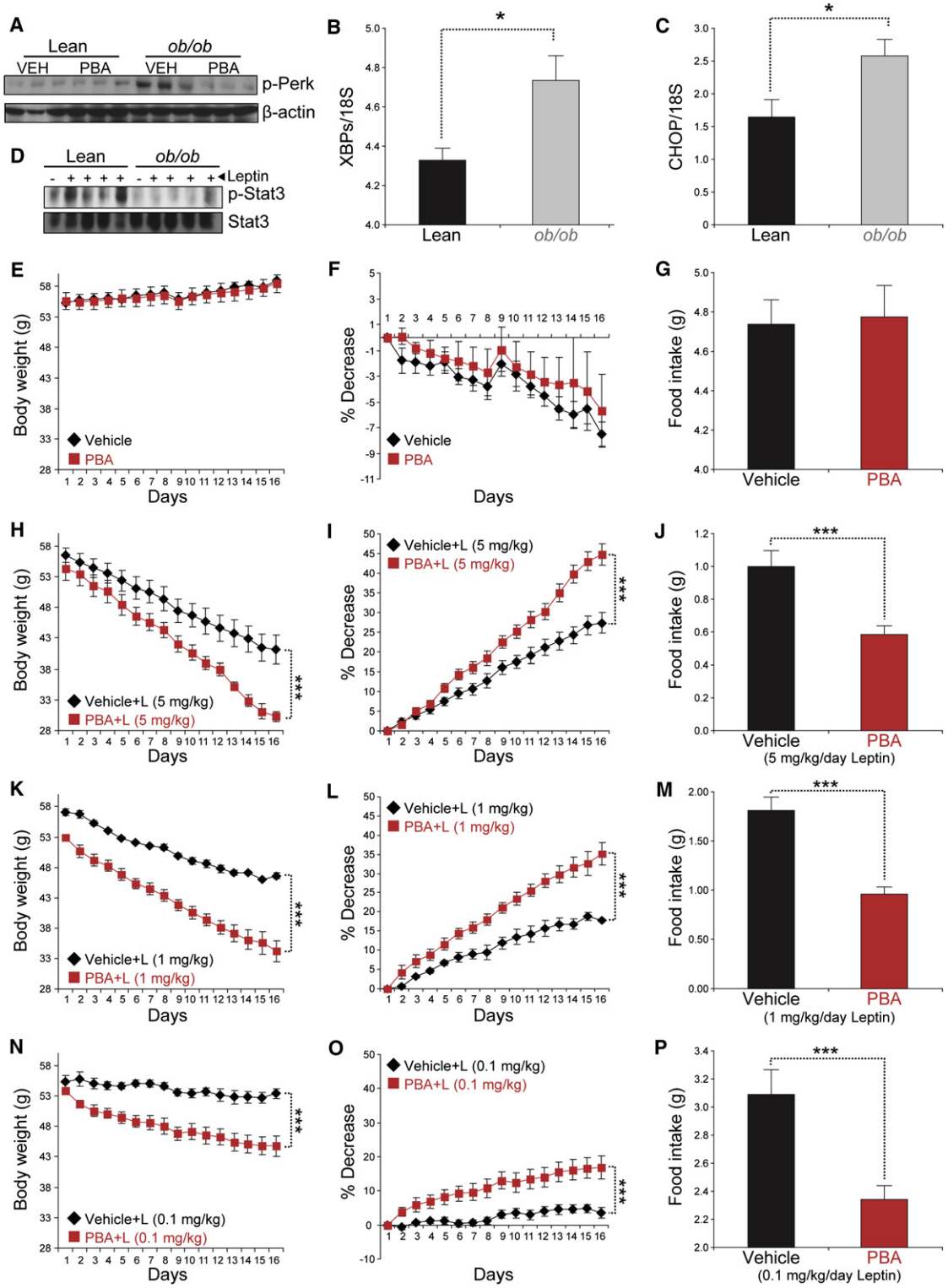

Figure 4. PBA Increases Leptin Sensitivity in the *ob/ob* Mice

(A) The 9-week-old lean WT and *ob/ob* mice were orally treated with either 4-phenyl butyrate (PBA) (1 g/kg/day) or vehicle (VEH) for 26 days, and PERK (Thr980) phosphorylation is examined in the hypothalamus extracts with direct immunoblotting.

(B and C) mRNA levels of (B) XBP1s and (C) CHOP in the hypothalamus of lean and *ob/ob* mice after 6 hr of fasting.

(D) The 10-week-old WT lean and *ob/ob* mice were intraperitoneally injected with leptin (0.1 mg/kg) after 6 hr starvation. Hypothalami were removed 30 min after the injections, and pStat3^{Tyr705} and total Stat3 levels were examined. (Experiments were repeated in two independent cohorts.) The 9-week-old lean WT and

Next, we performed metabolic cage analysis of XBP1$^{flox/flox}$ and *XNKO* groups. Parallel to the obesity phenotype, *XNKO* mice consume significantly less O_2 and produce a significantly lower amount of CO_2 (Figures 3K and 3L). Although there was a slight decrease in the respiratory exchange ratio in *XNKO* mice, this parameter was not statistically different (Figure 3M). In addition, *XNKO* mice are significantly less active in the dark cycle and over the total recording time (Figure 3N). Heat production does not differ between the groups (Figure 3O).

Insulin levels were also significantly upregulated during the course of HFD feeding (Figure S3A), and 6 hr fasted blood glucose of *XNKO* mice was significantly higher than control mice at the twelfth week of HFD (Figure 3P). Additionally, we performed GTT and ITT at weeks 10 and 12, respectively. *XNKO* mice were significantly more glucose intolerant than XBP1$^{flox/flox}$ control mice (Figure S3B). The hypoglycemic response to insulin was significantly blunted in the *XNKO* mice during the ITT (Figures S3C, S3D, and S3E). Furthermore, we investigated the response of *XBP1*$^{flox(-/-)}$/*NesCre*$^{(-/-)}$, *XBP1*$^{flox(+/+)}$/*NesCre*$^{(-/-)}$, and *XBP1*$^{flox(-/-)}$/*NesCre*$^{(+/-)}$ mice to high-fat diet feeding to examine whether there is any difference between these groups. During the 12 weeks of HFD feeding, body weight and other parameters did not show any significant alterations between the groups (Figure S4).

If development of a more severe form of obesity in *XNKO* mice is due to a higher level of ER stress and a consequent decrease in leptin signaling in the hypothalamus, then it would be expected that *XNKO* mice will have more ER stress and will be less sensitive to acute injection of leptin. To address these questions, we first analyzed the PERK phosphorylation in the hypothalamus of the *XNKO* and XBP1$^{flox/flox}$ mice after 12 weeks of HFD feeding. As shown in Figure 3Q, PERK phosphorylation (Thr980) is markedly upregulated in the hypothalamus of the *XNKO* mice, and leptin-stimulated Stat3^{Tyr705} phosphorylation is significantly blunted in the *XNKO* mice (Figure 3R).

As a final step in characterization of the *XNKO* mice, we analyzed the pancreas histology by either hematoxylin and eosin (H&E) or insulin/glucagon immunofluorescence stainings. There is a marked hyperplasia in the islets of the *XNKO* mice (Figure S5A). In addition, PERK phosphorylation is both increased in the liver and adipose tissues of the *XNKO* mice when compared with the XBP1$^{flox/flox}$ control mice Figures S5B and S5C).

Collectively, our results support the hypothesis that ER capacity of the brain is a crucial regulator of body weight, leptin sensitivity, and, thus, metabolic homeostasis.

Chemical Chaperones Are Leptin Sensitizers

Chemical chaperones constitute a group of low-molecular-weight compounds that have been shown to increase ER function and decrease the accumulation and aggregation of misfolded proteins in the ER lumen and, consequently, reduce ER stress (Perlmutter, 2002). 4-phenyl butyrate (PBA) and tauroursodeoxycholic acid (TUDCA) are U.S. Food and Drug Administration (FDA)-approved chemical chaperones and have high safety profile in humans (Chen et al., 1997; Maestri et al., 1996). Recent evidence suggests that PBA and TUDCA relieve ER stress in liver and adipose tissues, enhance insulin sensitivity, and maintain euglycemia in a mouse model of severe obesity and type 2 diabetes (*ob/ob*) (Ozcan et al., 2006). PBA and TUDCA also exert chaperone activity within the CNS (Inden et al., 2007; Petri et al., 2006; Sola et al., 2003). Considering these findings, we asked whether we could reverse ER stress in the hypothalamus of the obese mice by chemical chaperone treatment and, consequently, use this strategy to increase leptin sensitivity.

Ob/ob mice are known to respond to high levels of leptin. If our view, which implies that obesity conditions or the conditions that are leading to obesity create ER stress and, consequently, leptin resistance, is a valid one, then ER stress should also be upregulated in the hypothalamus of the *ob/ob* mice, and this should create at least some degree of leptin resistance, which, in turn, should be ameliorated by the blockade of UPR signaling. Indeed, the phosphorylation of PERK (Thr980) is increased in the hypothalamus of the *ob/ob* mice, indicating that ER stress is increased when compared to lean counterparts (Figure 4A). Furthermore, administration of PBA significantly reduced PERK phosphorylation, constituting evidence that hypothalamic ER stress can be modulated with PBA (Figure 4A). In addition, we analyzed mRNA levels of XBP1s and CHOP in the hypothalamus of lean and *ob/ob* mice after 6 hr fasting during the light cycle and demonstrated that both of the markers are significantly upregulated in the hypothalamus of the *ob/ob* mice when compared with the lean counterparts (Figures 4B and 4C).

After showing that UPR signaling is activated in the hypothalamus of the *ob/ob* mice, we sought to determine whether there is any difference in response of the *ob/ob* mice to leptin in terms of activating the LepRB signaling cascade in the hypothalamus. We intraperitoneally injected low doses (compared to the commonly used doses) of leptin (0.1 mg/kg) to aged-matched male WT and *ob/ob* mice at 6 hr fasting and extracted the hypothalamus 30 min after the injections. As shown in Figure 4D, WT lean mice responded well to this dose of leptin by increasing the Stat3^{Tyr705} phosphorylation in the hypothalamus. In contrast, this response is completely absent in the *ob/ob* mice, indicating that *ob/ob* mice have some degree of defect in activating the leptin-signaling pathway when compared with the WT mice (Figure 4D).

To test whether reduction of ER stress will increase leptin sensitivity of the *ob/ob* mice, we orally administered PBA or vehicle for 10 days as a pretreatment. Following this period, daily leptin injections (IP) were given at doses ranging from

ob/ob mice were orally treated with PBA (1 g/kg/day) for 10 days. Following the pretreatment period, leptin-deficient *ob/ob* mice were either administered with VEH or with different doses of leptin through the intraperitoneal route.

(E–G) The effect of VEH or PBA administration on (E) body weight (g), (F) percent decrease in body weight, and (G) 24 hr food intake (n = 3 for VEH, and n = 4 for PBA-treated group).

(H–J) Effect of 5 mg/kg/day leptin administration on (H) body weight, (I) percent decrease in body weight, and (J) 24 hr food intake in VEH- or PBA-treated *ob/ob* mice (n = 3 for VEH, and n = 4 for PBA-treated group).

(K–P) Analysis of the same parameters (body weight, percent decrease in body weight, and 24 hr food intake) in (K)–(M) 1 mg/kg/day and (N)–(P) 0.1 mg/kg/day leptin-treated mice (n = 3 for VEH, and n = 4 for PBA-treated group).

Data presented as means ± SEM. *p < 0.05, **p < 0.01, ***p < 0.001.

0.01 mg/kg/day to 5 mg/kg/day. Oral PBA administration did not affect the body weight or food consumption as compared to the vehicle-treated group alone (Figures 4E, 4F, and 4G). In the vehicle-treated group, the highest dose of leptin (5 mg/kg/day) significantly inhibited food intake (Figure 4H) and, during 16 days of treatment, reduced body weight from 56 ± 1.16 g to 41.13 ± 2.35 g (Figure 4F), a 27.33% decrease in the body weight (Figure 4G). However, in the PBA-treated group, the same (5 mg/kg/day) dose of leptin further inhibited food intake and reduced body weight from 54.30 ± 1.40 g to 30.30 ± 0.82 g (Figure 4F), corresponding to a 44.73% ± 2.55% decrease from the initial weight. This reduction was significantly greater than that seen in the vehicle-treated group (44.73% ± 2.55% versus 27.33% ± 2.65%, PBA versus vehicle, $p < 0.0001$).

Furthermore, PBA pretreatment dramatically increased the sensitivity of *ob/ob* mice to the anorexigenic effect of lower doses of leptin (1 mg/kg/day or 0.1 mg/kg/day). Following vehicle pretreatment, 1 mg/kg/day leptin treatment led to a significant decrease in body weight, albeit to a lesser extent than that seen at 5 mg/kg/day, by reducing the initial weight from 57.10 ± 0.58 g to 46.61 ± 0.52 g (17.73% reduction in body weight) (Figure 4I). However, following PBA pretreatment, the same 1 mg/kg/day leptin dose reduced body weight from 52.93 ± 0.26 g to 34.21 ± 1.74 g, corresponding to a 35.21% decrease in body weight ($p < 0.001$) (Figure 4I). At the lowest dose (0.1 mg/kg/day), leptin alone did not significantly reduce the body weight (Figure 4I). However, when *ob/ob* mice were pretreated with PBA, 0.1 mg/kg/day leptin decreased body weight from 53.82 ± 0.4 g to 44.77 ± 1.67 g, corresponding to a 16.77% decrease in body weight, which is commensurate with the level created by vehicle plus 1 mg/kg/day leptin, a 10-fold higher dose (Figure 4J). We also analyzed the blood glucose levels of the vehicle, leptin (5 mg/kg/day), PBA, and PBA + leptin-treated (5 mg/kg/day) *ob/ob* mice. When the *ob/ob* mice were treated with PBA and leptin together, blood glucose levels decreased to 91 ± 15 mg/dl, which is significantly lower than the PBA and leptin treatments alone. In addition, we treated the male and age-matched lean C57BL/6 mice with the same combination of leptin doses and PBA. As shown in Figure S6, PBA itself did not decrease the body weight and food consumption (Figures S6A–S6I).

To investigate whether the effect created by PBA and leptin combinatory treatment is solely mediated through the LepRB and is not due to a nonspecific effect, we performed the same experiment in the *db/db* mouse model, which lacks the leptin receptor. During the 16 days of experimental period, vehicle and PBA-treated groups significantly gained weight (Figures 5A and 5B), and there was no difference in the amount of food consumption between the vehicle and PBA-treated *db/db* mice. However, blood glucose levels of PBA-treated *db/db* mice were reduced to a significantly lower level, indicating that PBA is also capable of increasing insulin sensitivity in the *db/db* obesity model (Figure 5D). As expected, leptin treatment alone did not decrease the food intake and body weight of the *db/db* mice (Figures 5A, 5B, and 5C). Coadministration of leptin with PBA did not also change any of the parameters (increase in body weight, food consumption) (Figures 5A, 5B, and 5C), indicating that the leptin-sensitizing effect of PBA is solely mediated by the leptin receptor, but not through other possible signaling pathways, including the insulin receptor signaling.

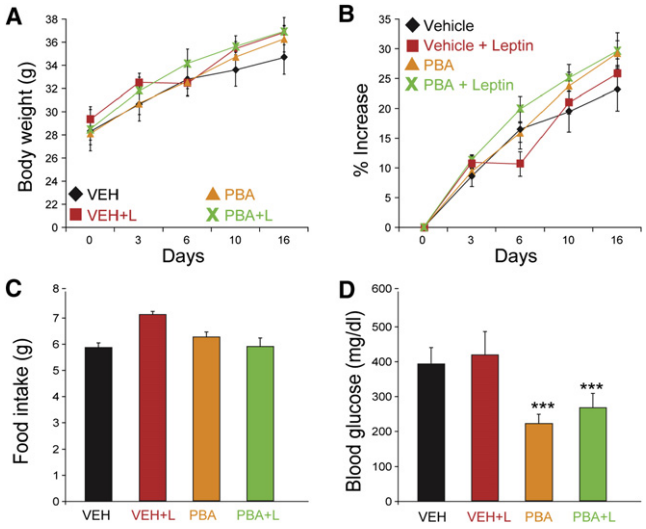

Figure 5. PBA and Leptin Coadministration in *db/db* Mouse Model

The 6-week-old *db/db* mice were orally treated with either PBA (1 g/kg/day) or VEH for 4 days. Following the pretreatment period, leptin-receptor-deficient *db/db* mice were either administered with VEH or leptin (1 mg/kg) through intraperitoneal route for 16 days.

(A–C) (A) Body weight (g), (B) percent increase in body weight, and (C) 24 hr food intake.

(D) Blood glucose (mg/dl) levels of the groups (n = 5 in each group).

Error bars, ± SEM. p values are determined by Student's t test. *$p < 0.05$, **$p < 0.01$, ***$p < 0.001$.

Obesity owing to a high-fat diet is fundamentally different from that seen in *ob/ob* mice in that it occurs in the face of high leptin levels. To determine whether PBA also sensitizes HFD-fed obese mice to leptin, mice that were kept on HFD for 25 weeks were pretreated with vehicle or PBA for 10 days and then given leptin treatment (5 mg/kg/day). Leptin administration to the vehicle-treated group led to an acute weight loss, which was rapidly regained (Figure 6A). By the end of treatment period, leptin created a slight but significant change in the body weight in the vehicle-treated group by reducing it from 42.42 ± 0.27 g to 40.78 ± 0.55 g (3.8% ± 0.9% decrease in body weight) (Figures 6A and 6B). However, PBA pretreatment increased the efficacy of leptin by significantly decreasing the daily food intake (Figure 6C) and leading to a 15.72% ± 2.85% reduction in body weight by reducing the initial weight from 41.18 ± 0.49 g to 34.71 ± 0.69 g (Figures 6A and 6B). During the course of the experiment, we placed the vehicle and PBA-treated groups in metabolic cages to investigate metabolic homeostasis in detail. As shown in Figure 6D, PBA treatment significantly increased leptin-stimulated O_2 consumption. It also led to an increase in CO_2 production (Figure 6E), but not at a significant level. At the dark cycle and in total recording time, activity of the PBA + leptin-treated mice significantly increased when compared with the leptin-treated group alone (Figure 6F). The respiratory exchange ratio in the PBA-treated group was significantly reduced in the dark cycle and also slightly in the light cycle (Figure 6G). In addition, heat production also shows slight upregulation in the PBA + leptin-treated mice (Figure 6H). Following the metabolic cage analysis, we performed DEXA scan to analyze whole-body fat

content. The lean mass does not change in both of the groups (Figure 6I). However, fat percentage and total fat amount is significantly reduced in PBA + L group (Figures 6J and 6K).

To investigate whether PBA treatment reduces the ER stress, we analyzed the PERK phosphorylation in the HFD-fed mice, which were either treated with VEH or PBA for 16 days. PBA treatment alone did not reduce the body weight and food intake when compared with the VEH-treated group (Figure S7). However, as shown in Figure 6I, PBA treatment led to a marked decrease in PERK phosphorylation in the hypothalamus of the HFD-fed obese mice, indicating that ER stress is reduced. To investigate whether leptin-stimulated activation of LepRB signaling is increased in the hypothalamus of the PBA-treated, HFD-fed obese mice, we intraperitoneally injected leptin (0.75 mg/kg) following a 6 hr fast and analyzed the Stat3^{Tyr705} phosphorylation in the hypothalamus extracts of VEH and PBA-treated mice. PBA treatment led to a marked upregulation in leptin-stimulated Stat3^{Tyr705} phosphorylation (Figure 6M). Treatment of ND-fed lean mice with PBA did not cause a higher activation of Stat3^{Tyr705} when compared with the VEH-treated group (Figure 6N). Collectively, these data provide evidence that PBA is effective in genetic and diet-induced obesity models as a leptin sensitizing agent.

Leptin resistance in obesity arises due to both impairment of leptin action in the hypothalamus and defects in the transport of leptin in the blood brain barrier (Banks, 2003; Flier, 2004). To investigate whether PBA treatment caused a generalized increase in the blood brain barrier permeability, we treated the HFD-fed WT male mice with PBA for 12 days and then injected with the retrogradely transported marker substance Fluoro-gold (IP, 15 mg/kg). As shown in Figure S8, there is Fluoro-gold immunostaining in the median eminence (ME) of both VEH and the PBA-treated mice. Reactivity against the Fluoro-gold is not different between the vehicle and PBA-treated groups. Fluoro-gold-labeled neurons should be present in the areas like ventromedial hypothalamus (VMH), dorsomedial hypothalamus (DMH), and lateral hypothalamic area (LHA) if the BBB permeability is perturbed. However, we did not observe any Fluoro-gold-labeled neurons in these areas, indicating that BBB permeability is not increased with the use of PBA (Figure S8).

If the postulate that reduction of ER stress in the hypothalamus increases leptin sensitivity is true, chemical chaperones other than PBA should also create the same effect and sensitize the obese mice to leptin. TUDCA is a hydrophilic bile acid, which has a completely different structure than PBA but has chemical chaperone activity in common (Ozcan et al., 2006). First, we investigated whether TUDCA can reduce ER stress in the hypothalamus of the *ob/ob* mice. For this purpose, we treated *ob/ob* mice either with vehicle or TUDCA (150 mg/kg/day) for a period of 21 days and analyzed the hypothalamic PERK phosphorylation. TUDCA treatment, similar to PBA, downregulated the PERK activity, indicating that TUDCA is also capable of reducing ER stress in the hypothalamus of the *ob/ob* mice. Taking this data into account, we asked whether TUDCA might also act as a leptin-sensitizing agent. To address this question, we first pretreated the *ob/ob* mice with TUDCA (150 mg/kg/day) for 5 days and subsequently initiated leptin (1 mg/kg) treatment. As shown in Figure 7B, neither TUDCA nor the vehicle alone increased the body weight of the *ob/ob* mice. Leptin treatment decreased the body weight from 50.50 ± 0.55 g to 43.75 ± 0.22 g, which corresponds to a 9.27% ± 1.34% reduction from the initial value. Body weight of the *ob/ob* mice decreased further with leptin and TUDCA cotreatment and reached 34.39 ± 1.30 g from 50.55 ± 1.14 g (25.14% ± 1.83% decrease, Lep versus TUD + Lep, $p < 0.001$). In addition, we investigated the daily food intake and showed that administration of leptin together with TUDCA significantly augments the appetite-suppressing effect of leptin (Figure 7D). Administration of TUDCA lowered the blood glucose levels, and addition of leptin to the treatment slightly reduced the blood glucose levels further (Figure 7E). Furthermore, to investigate the metabolic homeostasis in greater detail, we placed the mice in metabolic cages. As shown in Figures 7F and 7G, cotreatment with TUDCA and leptin increased CO_2 production and O_2 consumption. The respiratory exchange rate in the dark cycle showed slight downregulation, but not at a significant level (Figure 7H). The total activity of the TUDCA- and leptin-cotreated group was significantly higher than the leptin-only-treated group (Figure 7I). Heat generation was the same between the groups (Figure 7J). Next, we analyzed the whole-body fat composition by DEXA scan. TUDCA and leptin cotreatment led to a severe reduction in total fat amount and whole-body fat percentage, which are both significantly lower than the leptin-treated group alone (Figures 7K and 7L). Finally, analysis of lean mass has shown that none of the treatments lead to a significant change in this parameter (Figure 7M). We additionally investigated the effect of TUDCA and leptin cotreatment on C57BL/6 WT-lean mice (Figures S9A, S9B, and S9C).

We next tested the efficacy of TUDCA as a leptin sensitizer in the HFD-induced obesity model. In this experiment, we used 35-week-old and C57BL/6 WT mice, which were kept on HFD feeding for 32 weeks. We divided the mice into two groups for TUDCA and TUDCA-leptin cotreatment. Body weight of the mice in this cohort was between 35 and 52 g. We specifically chose the mice with the highest body weight for the TUDCA and leptin cotreatment group to investigate whether leptin will become effective in these severely obese mice when administered along with the TUDCA. The initial body weight of the TUDCA group was 38.33 ± 1.16 g, and the TUDCA + leptin group was 48.46 ± 1.82 g (Figure 7N). Following an initial 5 days acclimation period, mice were treated with TUDCA (150 mg/kg/day) for 4 days, and, subsequently, either vehicle or TUDCA treatment was started. Following the acclimation, TUDCA pretreatment was started, and following the 5 day pretreatment, vehicle and leptin (1 mg/kg/day) administration were initiated. TUDCA alone led to a significant decrease in body weight by reducing the initial weight from 36.16 ± 0.99 g to 32.61 ± 0.65 during the 16 days of treatment period (Figures 7N and 7O). Incapability of TUDCA in lowering the body weight of *ob/ob* (Figure 7B) or WT lean mice (Figure S9A) strongly indicates that TUDCA increases leptin sensitivity in such a way that endogenous high levels of leptin become effective. Indeed, in our experience, TUDCA acts as a much more powerful chemical chaperone when compared to PBA, as doses of TUDCA necessary for reducing ER stress in cellular systems (Ozcan et al., 2006) or as a leptin-sensitizing agent are much lower than for PBA. For example, administration of 50 mg/kg/day TUDCA to the *ob/ob* mice also significantly sensitizes this model to leptin. When administered with 50 mg/kg/day TUDCA, leptin's body-weight-reducing effect is

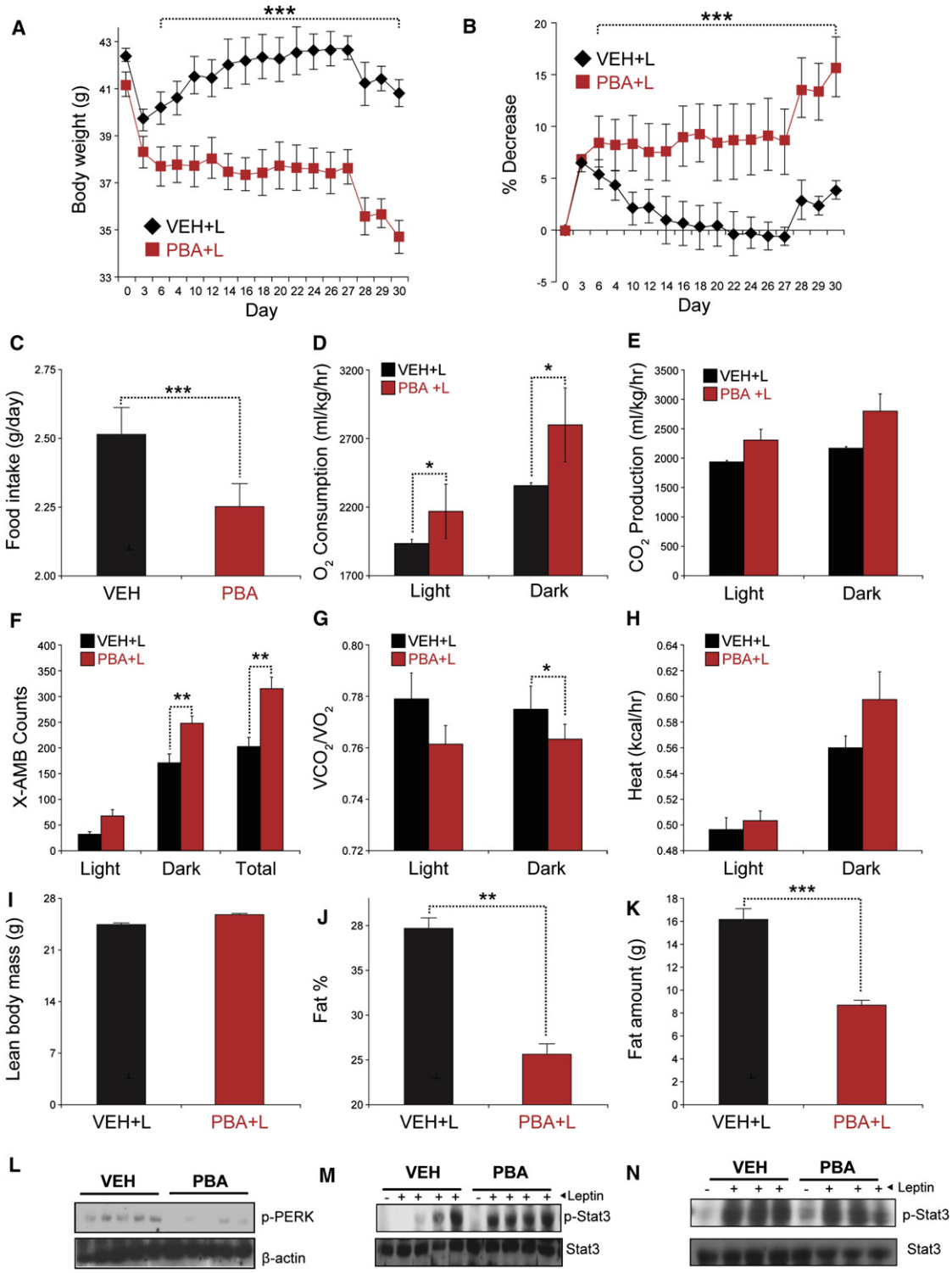

Figure 6. Effect of PBA on the Leptin Sensitivity of Diet-Induced Obese Mice

C57BL/6 mice that were kept on high-fat diet feeding for 25 weeks were either treated with vehicle or PBA (1 g/kg/day) for 10 days. Following the pretreatment period, mice were given daily leptin (5 mg/kg/day, IP) treatment.

(A–H) (A) Body weight (g), (B) percent of decrease in the body weight, and (C) 24 hr food intake (g) during the 30 days of leptin administration. Metabolic cage analysis was performed after 25 days of treatment. (D) O_2 consumption (ml/kg/hr), (E) CO_2 production (ml/kg/hr), (F) x axis ambulatory activity, (G) respiratory exchange ratio (VCO_2/VO_2), (H) heat generation (kcal/hr).

(I–K) Dexa scan analysis of (I) lean body mass (g), (J) fat percentage, and (K) total fat amount (g). C57BL6 mice were fed a HFD for a period of 25 weeks and then either treated with PBA (1 g/kg) or VEH for 16 days.

significantly more than the leptin alone (Lep versus TUD [50 mg/kg/day] + Lep, 9.27% ± 1.34% versus 15% ± 0.87%, $p < 0.001$). The limited efficacy of PBA could be the underlying reason for PBA's inability alone to decrease the body weight in the HFD-induced obesity model, since the leptin amount in the circulation may not be enough to overcome the remaining leptin resistance after the PBA treatment. Indeed, the leptin levels are significantly reduced after TUDCA, but not after 4-PBA treatment (Figure S10). Finally, coadministration of TUDCA and leptin generated a robust effect and reduced the body weight of HFD-fed obese mice from 45.19 ± 1.95 g to 35.61 ± 1.93 g, which is equal to an 18.88% decrease (Figures 7N and 7O) (TUD versus TUD + Lep, $p < 0.001$).

When our data is taken together, we believe that we can safely postulate that chemical chaperones or the agents, which have the ability to decrease ER stress, are leptin sensitizers. However, it is in the meantime possible that unknown effects of PBA and TUDCA other than decreasing ER stress may also contribute to increased leptin sensitivity.

DISCUSSION

Obesity is an escalating problem that constitutes a major threat to global human health. An alarming increase in the incidence of obesity among the pediatric population casts the disease into a new and more concerning dimension (Narayan et al., 2003; Rocchini, 2002). Although urgent therapeutic interventions are needed, effective therapeutic modalities to cure or prevent the development of obesity are limited.

In the present work, we have demonstrated that obesity creates ER stress and initiates the unfolded protein response signaling pathways in the hypothalamus, which, in turn, leads to inhibition of leptin receptor signaling and creation of leptin resistance. Our observations in the cellular systems exclude the possibility of a defect in LepRB folding in ER stress conditions, since translocation of LepRB to the membrane is not altered. It is surprising that binding of leptin to LepRB increases when cells are experiencing ER stress. This could be due to decreased LepRB internalization after binding of leptin in ER stress conditions. In addition, acute generation of ER stress in the hypothalamus of lean mice creates a phenotype similar to that seen in the brain of the obese mice. Tunicamycin infusion to the third ventricle increases AgRP and NPY levels and completely blocks leptin-stimulated Stat3 activation. In a heterologous cell system, enhancement of ER capacity leads to a robust leptin-stimulated LepRB activation, suggesting that ER capacity is directly related to the leptin sensitivity. Providing additional support to this hypothesis, we demonstrated that neuronal deletion of XBP1 and a consequent reduction in ER function creates severe ER stress in the hypothalamus, blocks leptin action, and generates leptin resistance in mice. The rapid and marked increase in the levels of circulating leptin in the neuronal XBP1-deficient mice upon HFD feeding indicates an earlier onset of a higher level of leptin resistance. In complete agreement with the leptin resistance phenotype, the *XNKO* mice consume more food, move significantly less, gain more weight, and develop significantly higher levels of adiposity and obesity. Increases in the leptin levels in obesity have been thought to be proportional to and the result of increased adiposity. Our results suggest that this might not always be the case, since regression analysis demonstrates that leptin levels and adiposity dissociate in the *XNKO* mice.

While all of the results discussed above provided support to the hypothesis that ER stress plays a role in the development of leptin resistance, they also raised a crucial question of whether the hypothalamic ER stress might be reduced with chemicals and whether this could be utilized as a strategy to sensitize obese mice and humans to the anorexigenic effect of leptin. Chemical chaperones have been previously demonstrated to be effective in reducing ER stress in different settings, including peripheral tissues in obesity (Ozcan et al., 2006), cystic fibrosis, and α1-antitrypsin deficiency (Perlmutter, 2002). PBA and TUDCA, which are the well-known members of the chemical chaperone family, also have the ability to reduce ER stress in the brain. They have been previously implicated as neuroprotective agents in the neurodegenerative diseases, where ER stress is considered to be one of the triggering mechanisms for the pathology (Inden et al., 2007; Petri et al., 2006).

We have shown that PBA and TUDCA pretreatment increase the leptin sensitivity of both genetic and diet-induced obesity models. Although high-dose leptin robustly reduces the body weight of the *ob/ob* mice, at lower doses, such as 0.1 mg/kg/day, it is minimally effective. PBA coadministration with either high or low doses of leptin augments the efficacy of leptin. For example, coadministration of PBA with only 0.1 mg/kg/day leptin provides equivalent weight loss to that seen with 1 mg/kg/day leptin alone, which could be defined as a 10-fold sensitization. It is also important to note that there is also some degree of ER stress in the *ob/ob* mice, and, when they are treated with the chemical chaperones, leptin efficacy dramatically increases. *Ob/ob* mouse model of obesity has always been accepted as a highly leptin-sensitive mouse model, since leptin administration does decrease the body weight and suppress the hyperphagia. However, the leptin doses that are necessary to suppress appetite and decrease the body weight are at supraphysiological levels. The leptin levels in a WT-lean mouse range between 1 and 4 ng/ml. If we hypothetically think about a 50 g mouse, which is as leptin sensitive as the WT-lean mouse, the total amount of leptin that would be sufficient to keep the body weight and hyperphagia under control in whole circulation (4–5 ml of blood) would be 20 ng. Although 0.1 mg/kg leptin accounts for 5000 ng of leptin for a 50 g mouse, this dose is not capable of decreasing the body weight of a 50 g *ob/ob* mouse. The maximum efficiency is seen between 1 and 5 mg/kg of leptin dose. These doses are 2500

(L) PERK phosphorylation in the hypothalamus extracts.
(M) Leptin-stimulated $Stat3^{Tyr705}$ phosphorylation in the VEH and PBA-treated HFD-fed mice.
(N) C57BL6 mice were fed a ND for a period of 25 weeks and then either treated with PBA (1 g/kg) or VEH for 16 days. Following the treatment period, mice were starved for 6 hr and subsequently injected with leptin (IP, 1 mg/kg). $Stat3^{Tyr705}$ phosphorylation and total Stat levels were examined in the hypothalamus extracts (n = 6 in each group).
Error bars, ± SEM. p values are determined by Student's t test. *$p < 0.05$, **$p < 0.01$, ***$p < 0.001$.

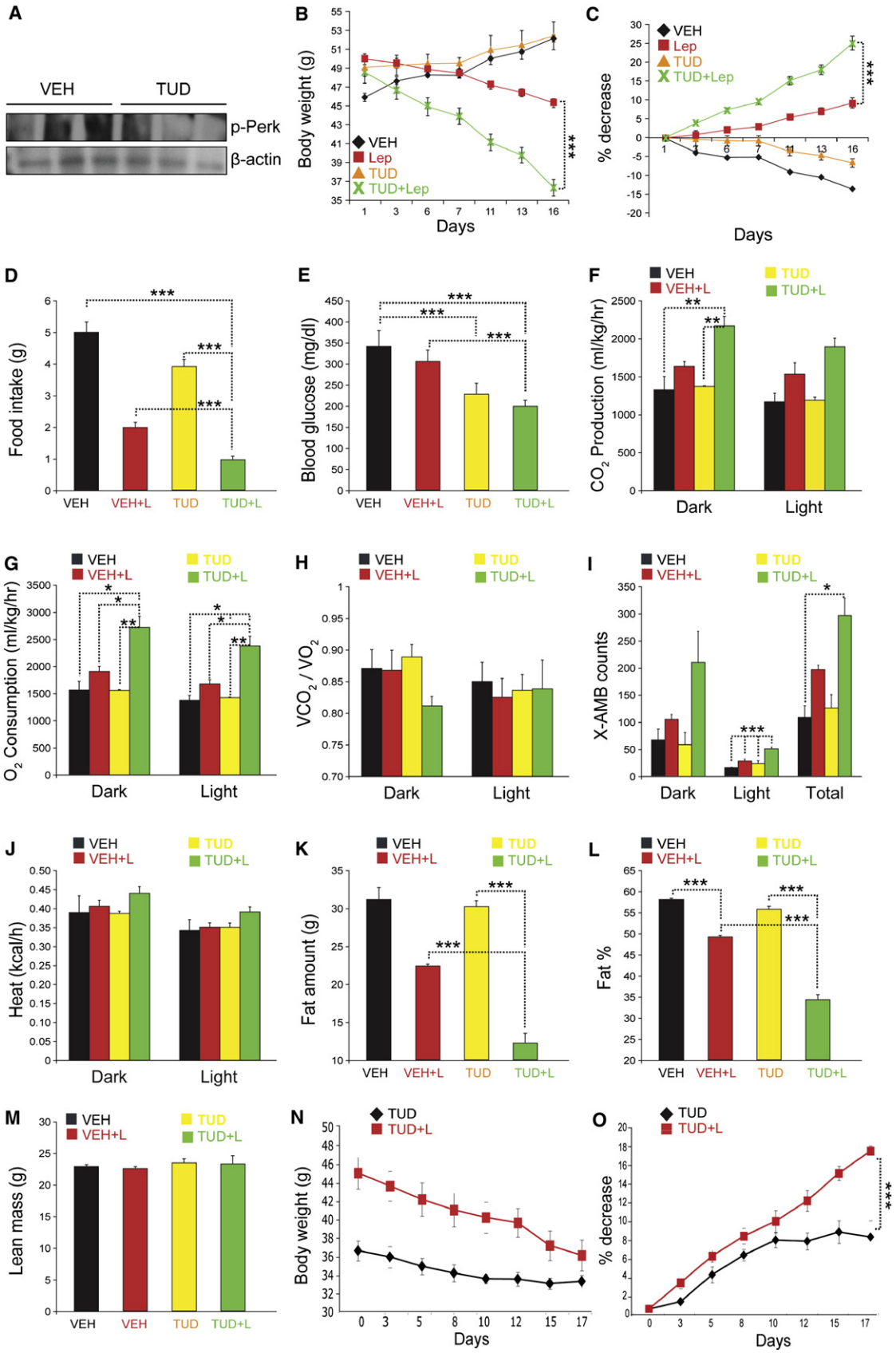
A
VEH
TUD
p-Perk
β-actin
B
Body weight (g)
VEH
Lep
TUD
TUD+Lep
***
Days
C
% decrease
VEH
Lep
TUD
TUD+Lep
***
Days
D
Food intake (g)
***
***
***
VEH
VEH+L
TUD
TUD+L
E
Blood glucose (mg/dl)
***
***
***
VEH
VEH+L
TUD
TUD+L
F
CO2 Production (ml/kg/hr)
VEH
VEH+L
TUD
TUD+L
**
**
Dark
Light
G
O2 Consumption (ml/kg/hr)
VEH
VEH+L
TUD
TUD+L
Dark
Light
H
VCO2 / VO2
VEH
VEH+L
TUD
TUD+L
Dark
Light
I
X-AMB counts
VEH
VEH+L
TUD
TUD+L
***
Dark
Light
Total
J
Heat (kcal/h)
VEH
VEH+L
TUD
TUD+L
Dark
Light
K
Fat amount (g)
VEH
VEH+L
TUD
TUD+L
***
***
L
Fat %
VEH
VEH+L
TUD
TUD+L
***
***
M
Lean mass (g)
VEH
VEH+L
TUD
TUD+L
VEH
VEH
TUD
TUD+L
N
Body weight (g)
TUD
TUD+L
Days
O
% decrease
TUD
TUD+L
***
Days

and 5000 times more than the physiological doses, respectively. Indeed, administration of leptin at 0.1 mg/kg activates the leptin receptor signaling in the hypothalamus of WT-lean mice, whereas this effect is totally absent in the *ob/ob* mouse model. It is also evident in the previous reports that ob/ob mice have a degree of leptin resistance. For example, Mistry et al. (1997) have shown that ICV administration of 50 ng of leptin to *ob/ob* mice is minimally effective in suppressing the appetite, and they have administered 1 μg of leptin through the ICV route to obtain significant effects. That 1 μg of leptin is 50 times higher than the expected dose of total leptin in the circulation of a 50 g leptin-sensitive *ob/ob* mouse model. In addition, although 50 ng of leptin is almost three times the amount that would be expected to fully mediate leptin's effect, it did not at all increase O_2 consumption, which is one of the signatures of leptin action. To further discuss this issue, we would like to emphasize the insulin resistance of *ob/ob* mice. It is well established that *ob/ob* mice are severely insulin resistant. Administration of 1 IU/kg of insulin minimally activates the insulin receptor signaling and cannot lower the blood glucose levels efficiently. However, if *ob/ob* mice are administered with 10 IU/kg of insulin, they will probably face hypoglycemia. We think that a similar phenomenon holds for the leptin sensitivity in the *ob/ob* mice. One more example from other systems could be the insulin-deficient diabetes models both in mice and humans. STZ-diabetic mice and type 1 diabetic patients can develop insulin resistance despite absolute deficiency of insulin. Taking all of these phenomenons and the data presented in this study into account, we think that it is possible that overconsumption of nutrients could itself be a reason for development of leptin resistance independent of prolonged leptin action. Thus, our data challenge the current concept that prolonged leptin exposure due to hyperleptinemia is the initiative and underlying factor for development of leptin resistance in obese mice. This line of thinking favors the fact that increased adiposity and consequent hyperleptinemia decreases the leptin action and creates the leptin resistance. Our data raise the possibility that increased UPR signaling even before the onset of adiposity and hyperleptinemia might be creating leptin resistance, and it might be the underlying reason for development of leptin resistance, since the leptin levels of *XNKO* mice severely increase at the early phases of HFD feeding, which are not proportional to the body weight. It should be also noted that leptin levels reach to extremely high levels in *XNKO* mice during the late phases of HFD feeding. We could not find any mouse model reported to date whose leptin levels are as high as the *XNKO* mice.

While discussed observations above are providing new insights regarding leptin sensitivity, the most important point is the ability of both PBA and TUDCA to show the leptin sensitizer effect in the diet-induced obesity model. In HFD-induced obese mice, leptin administration leads to an initial reduction in body weight, but this weight loss is rapidly regained, rendering leptin as an ineffective antiobesity drug. However, pretreatment of these mice with the PBA leads to a significant weight loss, showing that the effect that is seen in *ob/ob* mice also is also obtained in wild-type, diet-induced obese mice. Having shown that TUDCA, another chemical chaperone with a completely different structure than PBA, also increases leptin sensitivity in the *ob/ob* and HFD-fed mice provides important evidence that chemical chaperones in common are leptin sensitizers.

A leptin-sensitizing agent has not been previously described despite the long-standing efforts in both academia and industry. The results presented in this study provide evidence that chemical chaperones, particularly the PBA and TUDCA, can be used as leptin-sensitizing agents. When the high safety profiles of PBA, TUDCA, and leptin are taken into consideration, our results may define a novel treatment option for obesity.

EXPERIMENTAL PROCEDURES

Reagents

Phospho-Perk (Thr980), phospho-Stat3 (Tyr705), IRE1 antibodies were from Cell Signaling Technology (Beverley, MA). Phospho-tyrosine, Jak2, Stat3, and XBP1 antibodies were obtained from Santa Cruz Biotechnologies (Santa Cruz, CA). ATF6 was from Abcam (Cambridge, MA). Phospho-IRE1 antibody was from Novus Biologicals (Littleton, CO). BM chemiluminescence blotting substrate (POD) was from Roche Diagnostics, Inc. (Indianapolis, IN). PBA and Tunicamycin were from Calbiochem (San Diego, CA). Dulbecco's modified Eagle's medium (DMEM) was from GIBCO (Grand Island, NY). Humulin R was from Eli Lilly (Indianapolis, IN). TRIzol reagent and geneticin were from Invitrogen (Carlsbad, CA). iScript cDNA Synthesis Kit and Syber Green Fluoresence were obtained from Bio-Rad (Hercules, CA). Plastic cannulas were from Plastics One, Inc. (Wallingford, CT). Mouse recombinant leptin was commercially obtained from A.F. Parlow (Harbor-UCLA Medical Center). Mouse Leptin Elisa Kit and Ultra-Sensitive Mouse Insulin Elisa Kit were from Crystal Chem, Inc. (Downers Grove, IL).

Cell Culture and Signaling Experiments

Human 293 cells, which were stably transfected with LRb, were cultured in 5% CO_2 incubator in 150 cm^2 cell culture flasks in DMEM-H, which contains 10%

Figure 7. Chemical Chaperone TUDCA Also Acts as a Leptin Sensitizer

(A) Hypothalamic PERK phosphorylation (Thr980) after 21 days of vehicle or TUDCA (150 mg/kg/day) treatment. Following a 5 day pretreatment with TUDCA (150 mg/kg/day) or vehicle, 9- to 10-week old *ob/ob* mice were treated either with leptin (1 mg/kg/day) or vehicle.

(B–D) (B) Body weight (g), (C) percent of decrease in body weight, and (D) daily food intake of the *ob/ob* mice during 18 days of treatment period with the indicated regimens.

(E) Blood glucose (mg/dl) levels at the eighteenth day of treatment. Metabolic cage studies were performed.

(F) CO_2 production (ml/kg/hr).

(G) O_2 consumption (ml/kg/hr).

(H) Respiratory exchange ratio (VCO_2/VO_2).

(I) X axis ambulatory activity.

(J) Heat generation (kcal/hr).

(K–M) Dexa scan analysis of (K) total fat amount (g), (L) fat percentage, and (M) lean body mass (g).

(N) C57BL/6 male WT mice were kept on HFD feeding for 32 weeks and, following a 5 day acclimation period, were pretreated with TUDCA (150 mg/kg/day) for 5 days. At the end of the pretreatment period, intraperitoneal vehicle and leptin (1 mg/kg/day) treatments were started. (N) Body weight (g) and (O) percent of decrease in body weight of the HFD-fed mice during the 16 day treatment (n = 6 for VEH, n = 7 for Lep, n = 7 for TUD, and n = 8 for TUD + Lep group).

Error bars, ± SEM. p values are determined by Student's t test. *$p < 0.05$, **$p < 0.01$, ***$p < 0.001$.

fetal bovine serum (FBS), 1% penicillin-streptomycin complex, and 500 μg/ml geneticin. After reaching a 90% confluency, cells were passed to 10 cm^2 cell culture dishes at a confluency of 70%. Following 24 hr, cells were washed three times with DMEM-H medium, which does not contain FBS, and then taken into incubation with DMEM-H with 1% FBS. After 12–14 hr of incubation in this medium, cells were exposed to tunicamycin (3 μg/ml, 4 hr) and stimulated with leptin (100 ng/ml) for a period of 45 min. Tunicamycin is dissolved in DMSO, and stock concentration was 3 mg/ml. To reach to 3 ug/ml, it was diluted 1000 times. To have the appropriate control, the same amount of DMSO was added in 1/1000 dilution. At the end of leptin treatment, the medium was removed and cells were flash frozen in liquid nitrogen and kept in −80°C until further processing.

Analysis of PERK Phosphorylation in the Hypothalamus

Analysis of PERK phosphorylation in tissues is a difficult process, and extreme precautions are needed for successful detection. To analyze PERK phosphorylation in the hypothalamus, we have combined three hypothalamus and lysed them in 1 ml of tissue lysis buffer containing 25 mM Tris-HCl (pH 7.4), 10 mM Na3VO4, 100 mM NaF, 50 mM Na4P2O7, 10 mM EGTA, 10 mM EDTA, 1% NP-40, 10 ug/ml Leupeptin, 10 ug/ml Aprotinin, 2 mM PMSF, and 20 nM okadaic acid. Following denaturation in Laemmlie buffer, 300 μg of total protein was loaded into the wells of the 16 × 16 cm 6% SDS-PAGE gel, and electrophoresis was performed at 60 V over an 18 hr period. Electrophoresis buffer was two times changed to have uniform electrophoresis of the samples in the gel. Following the overnight transfer to the PVDF membrane (45 μM pore size), the blot has been incubated in blocking solution at room temperature for 1 hr and taken to overnight antibody incubation in 5% blocking solution at 1/1000 dilution at 4°C. Subsequently, the membranes were washed with TBST six times for 20 min and taken into secondary antibody incubation (1/5000 or 1/1000 dilution). Following the secondary antibody incubation, membranes were washed with TBST ten times for 20 min each, and, subsequently, membranes were exposed to the chemiluminisence substrate for developing the films. Usually more than 20 min of exposing has been necessary to obtain the p-PERK signal (in some of the experiments, we exposed the membranes ~2–~3 hr to detect the signal). In the experiments in which high exposure time has created nonspecific darkening of the films, which interfered with clearly visualizing the p-PERK signal, we have performed overnight washing and developed the films after this step.

Intracerebro-Ventricular Cannulation and Tunicamycin Infusion

The experiments were carried out on adult, male, 8- to 10-week-old WT (C57BL/6) mice. The WT mice were implanted with 26 gauge stainless steel guide cannula into the third ventricle under stereotaxic control using a stereotaxic apparatus (coordinates from Bregma: anteroventral, −1.8 mm; lateral, 0.0 mm; dorsoventral, 5.0 mm) through a hole created in the skull with a micro driller. The cannula was secured to the skull with Crazy Glue and dental cement and temporarily occluded with a dummy cannula. Triple antibiotic ointment containing Bacitracin was applied to the interface of the cement and the skin. Animals were weighed daily, and any animal showing signs of illness or weight loss was removed from the study and euthanized. At 7 days after ICV cannulation, WT mice were divided into two groups. The first group of WT (n = 4) mice was infused with 2 μl of DMSO as a vehicle, and the second group (n = 4) was infused with 2 μl of tunicamycin (40 mg/ml). All ICV injections were made through a 31 gauge needle that extended 0.5 mm below the guide cannula, connected by cannula connector to a 10 μl Hamilton syringe and infused over 3 min. After 5.5 hr, mice were intraperitoneally treated either with PBS or leptin (1 mg/kg). At 30 min after leptin administration, hypothalamus was dissected and flash frozen in liquid nitrogen and kept in −80°C until further processing. For gene expression analysis, hypothalami were dissected 12 hr after tunicamycin and vehicle infusion.

SUPPLEMENTAL DATA

The Supplemental Data for this article include Supplemental Experimental Procedures and ten figures and can be found with this article online at http://www.cell.com/cell-metabolism/supplemental/S1550-4131(08)00389-6.

ACKNOWLEDGMENTS

We thank Laurie H. Glimcher for kindly providing us with the $XBP1^{flox/flox}$ mouse strain. We thank Eric D. Smith for his editorial advice and help. We are indebted to Joseph A. Majzoub and Morris F. White for their continuous support and time for critical reading of our manuscript. We thank Kyle Copps for critical reading of our manuscript. We thank Mustafa M. Sahin for his kind advice and discussion of neuronal cell culture and hypothalamic explants experiments. We thank David Ron for providing us with the $PERK^{-/-}$ cells. This study was supported by junior faculty start-up funds and a Translational Research Award provided to U.O. from Children's Hospital Boston and from Timothy Murphy Funds provided to Division of Endocrinology, Children's Hospital Boston.

U.O. conceived the hypothesis, designed the experiments, performed the experiments, analyzed the data, and wrote the manuscript. L.O. performed experiments and analyzed data. A.S.E. provided help to U.O. and L.O. for performing experiments. S.S., A.L., and J.C. performed experiments. D.N. performed neuronal culture experiments. M.G.M., Jr. provided LepRB-expressing 293 cell line, LepRB antibody, and helpful comments and advice throughout the project.

Received: September 26, 2008
Revised: October 26, 2008
Accepted: December 5, 2008
Published: January 6, 2009

REFERENCES

Ahima, R.S., Prabakaran, D., Mantzoros, C., Qu, D., Lowell, B., Maratos-Flier, E., and Flier, J.S. (1996). Role of leptin in the neuroendocrine response to fasting. Nature *382*, 250–252.

Banks, W.A. (2003). Is obesity a disease of the blood-brain barrier? Physiological, pathological, and evolutionary considerations. Curr. Pharm. Des. *9*, 801–809.

Banks, W.A. (2004). The many lives of leptin. Peptides *25*, 331–338.

Bence, K.K., Delibegovic, M., Xue, B., Gorgun, C.Z., Hotamisligil, G.S., Neel, B.G., and Kahn, B.B. (2006). Neuronal PTP1B regulates body weight, adiposity and leptin action. Nat. Med. *12*, 917–924.

Bjorbak, C., Lavery, H.J., Bates, S.H., Olson, R.K., Davis, S.M., Flier, J.S., and Myers, M.G., Jr. (2000). SOCS3 mediates feedback inhibition of the leptin receptor via Tyr985. J. Biol. Chem. *275*, 40649–40657.

Chen, W.Y., Bailey, E.C., McCune, S.L., Dong, J.Y., and Townes, T.M. (1997). Reactivation of silenced, virally transduced genes by inhibitors of histone deacetylase. Proc. Natl. Acad. Sci. USA *94*, 5798–5803.

Elmquist, J.K., Elias, C.F., and Saper, C.B. (1999). From lesions to leptin: Hypothalamic control of food intake and body weight. Neuron *22*, 221–232.

Farooqi, I.S., and O'Rahilly, S. (2005). Monogenic obesity in humans. Annu. Rev. Med. *56*, 443–458.

Flier, J.S. (2004). Obesity wars: Molecular progress confronts an expanding epidemic. Cell *116*, 337–350.

Friedman, J.M., and Halaas, J.L. (1998). Leptin and the regulation of body weight in mammals. Nature *395*, 763–770.

Gao, Q., and Horvath, T.L. (2007). Neurobiology of feeding and energy expenditure. Annu. Rev. Neurosci. *30*, 367–398.

Halaas, J.L., Gajiwala, K.S., Maffei, M., Cohen, S.L., Chait, B.T., Rabinowitz, D., Lallone, R.L., Burley, S.K., and Friedman, J.M. (1995). Weight-reducing effects of the plasma protein encoded by the obese gene. Science *269*, 543–546.

Hetz, C., Lee, A.H., Gonzalez-Romero, D., Thielen, P., Castilla, J., Soto, C., and Glimcher, L.H. (2008). Unfolded protein response transcription factor XBP-1 does not influence prion replication or pathogenesis. Proc. Natl. Acad. Sci. USA *105*, 757–762.

Inden, M., Kitamura, Y., Takeuchi, H., Yanagida, T., Takata, K., Kobayashi, Y., Taniguchi, T., Yoshimoto, K., Kaneko, M., Okuma, Y., et al. (2007). Neurodegeneration of mouse nigrostriatal dopaminergic system induced by repeated

oral administration of rotenone is prevented by 4-phenylbutyrate, a chemical chaperone. J. Neurochem. *101*, 1491–1504.

Ishida-Takahashi, R., Rosario, F., Gong, Y., Kopp, K., Stancheva, Z., Chen, X., Feener, E.P., and Myers, M.G., Jr. (2006). Phosphorylation of Jak2 on Ser(523) inhibits Jak2-dependent leptin receptor signaling. Mol. Cell. Biol. *26*, 4063–4073.

Kloek, C., Haq, A.K., Dunn, S.L., Lavery, H.J., Banks, A.S., and Myers, M.G., Jr. (2002). Regulation of Jak kinases by intracellular leptin receptor sequences. J. Biol. Chem. *277*, 41547–41555.

Leibel, R.L., Chung, W.K., and Chua, S.C., Jr. (1997). The molecular genetics of rodent single gene obesities. J. Biol. Chem. *272*, 31937–31940.

Maestri, N.E., Brusilow, S.W., Clissold, D.B., and Bassett, S.S. (1996). Long-term treatment of girls with ornithine transcarbamylase deficiency. N. Engl. J. Med. *335*, 855–859.

Marciniak, S.J., and Ron, D. (2006). Endoplasmic reticulum stress signaling in disease. Physiol. Rev. *86*, 1133–1149.

Mistry, A.M., Swick, A.G., and Romsos, D.R. (1997). Leptin rapidly lowers food intake and elevates metabolic rates in lean and ob/ob mice. J. Nutr. *127*, 2065–2072.

Muoio, D.M., and Newgard, C.B. (2006). Obesity-related derangements in metabolic regulation. Annu. Rev Biochem. *75*, 367–401.

Myers, M.G., Jr. (2004). Leptin receptor signaling and the regulation of mammalian physiology. Recent Prog. Horm. Res. *59*, 287–304.

Myers, M.G., Jr. (2008). Metabolic sensing and regulation by the hypothalamus. Am. J. Physiol. Endocrinol. Metab. *294*, E809.

Narayan, K.M., Boyle, J.P., Thompson, T.J., Sorensen, S.W., and Williamson, D.F. (2003). Lifetime risk for diabetes mellitus in the United States. JAMA *290*, 1884–1890.

Ozcan, U., Cao, Q., Yilmaz, E., Lee, A.H., Iwakoshi, N.N., Ozdelen, E., Tuncman, G., Gorgun, C., Glimcher, L.H., and Hotamisligil, G.S. (2004). Endoplasmic reticulum stress links obesity, insulin action, and type 2 diabetes. Science *306*, 457–461.

Ozcan, U., Yilmaz, E., Ozcan, L., Furuhashi, M., Vaillancourt, E., Smith, R.O., Gorgun, C.Z., and Hotamisligil, G.S. (2006). Chemical chaperones reduce ER stress and restore glucose homeostasis in a mouse model of type 2 diabetes. Science *313*, 1137–1140.

Ozcan, U., Ozcan, L., Yilmaz, E., Duvel, K., Sahin, M., Manning, B.D., and Hotamisligil, G.S. (2008). Loss of the tuberous sclerosis complex tumor suppressors triggers the unfolded protein response to regulate insulin signaling and apoptosis. Mol. Cell *29*, 541–551.

Perlmutter, D.H. (2002). Chemical chaperones: A pharmacological strategy for disorders of protein folding and trafficking. Pediatr. Res. *52*, 832–836.

Petri, S., Kiaei, M., Kipiani, K., Chen, J., Calingasan, N.Y., Crow, J.P., and Beal, M.F. (2006). Additive neuroprotective effects of a histone deacetylase inhibitor and a catalytic antioxidant in a transgenic mouse model of amyotrophic lateral sclerosis. Neurobiol. Dis. *22*, 40–49.

Proulx, K., and Seeley, R.J. (2005). The regulation of energy balance by the central nervous system. Psychiatr. Clin. North Am. *28*, 25–38.

Rocchini, A.P. (2002). Childhood obesity and a diabetes epidemic. N. Engl. J. Med. *346*, 854–855.

Ron, D., and Walter, P. (2007). Signal integration in the endoplasmic reticulum unfolded protein response. Nat. Rev. Mol. Cell Biol. *8*, 519–529.

Scheuner, D., Vander Mierde, D., Song, B., Flamez, D., Creemers, J.W., Tsukamoto, K., Ribick, M., Schuit, F.C., and Kaufman, R.J. (2005). Control of mRNA translation preserves endoplasmic reticulum function in beta cells and maintains glucose homeostasis. Nat. Med. *11*, 757–764.

Schroder, M., and Kaufman, R.J. (2005). The mammalian unfolded protein response. Annu. Rev. Biochem. *74*, 739–789.

Schwartz, M.W., and Morton, G.J. (2002). Obesity: Keeping hunger at bay. Nature *418*, 595–597.

Schwartz, M.W., Woods, S.C., Porte, D., Jr., Seeley, R.J., and Baskin, D.G. (2000). Central nervous system control of food intake. Nature *404*, 661–671.

Sola, S., Castro, R.E., Laires, P.A., Steer, C.J., and Rodrigues, C.M. (2003). Tauroursodeoxycholic acid prevents amyloid-beta peptide-induced neuronal death via a phosphatidylinositol 3-kinase-dependent signaling pathway. Mol. Med. *9*, 226–234.

Stein, C.J., and Colditz, G.A. (2004). The epidemic of obesity. J. Clin. Endocrinol. Metab. *89*, 2522–2525.

Zhang, X., Zhang, G., Zhang, H., Karin, M., Bai, H., and Cai, D. (2008). Hypothalamic IKKbeta/NF-kappaB and ER stress link overnutrition to energy imbalance and obesity. Cell *135*, 61–73.